Anal. Chem. **2004,** *76,* 7234−7242

Molecular Depth Profiling of Histamine in Ice Using a Buckminsterfullerene Probe

Andreas Wucher,*,† Shixin Sun,‡ Christopher Szakal,‡ and Nicholas Winograd‡

Department of Chemistry, The Pennsylvania State University, 184 MRI Building, University Park, Pennsylvania 16802, and Physics Department, University of Duisburg−Essen, 45117 Essen, Germany

We employ a buckminsterfullerene ion source to probe the distribution of histamine molecules at the water-ice/vacuum interface. The experiments utilize secondary ion mass spectrometry to detect molecular ions that are desorbed from a frozen aqueous histamine solution. The results show that this cluster ion probe induces an extraordinarily high sputter yield of 2400 ice molecules per impact event as determined by a quartz crystal microbalance. As a consequence of this high yield, we show that it is possible to produce molecular depth profiles of the top several hundred nanometers below the ice surface without destruction of the molecular ion signal by accumulation of beam-induced chemical damage. Similar profiles are reported for desorbed neutral molecular fragments by utilizing a high-power femtosecond-pulsed laser for photoionization. While this type of information could not be achieved using atomic projectiles, it is possible to remove the damage induced by such projectiles by subsequent cluster bombardment. These experiments are particularly important for organic surface analysis since they suggest that cluster ion probes may successfully be employed to remove overlayers that may mask the desired molecular information in static secondary ion mass spectral analysis.

Energetic ion beams are unique tools for characterizing the near-surface composition of solids. Such compositions are determined by the beam-induced erosion of the surface layers, followed by analysis of the flux of desorbed atoms, usually with secondary ion mass spectrometry (SIMS). This strategy has been successful for locating atomic species such as dopant layers in semiconductor devices or evaluating the integrity of multilayer thin-film structures. Measurements may be obtained with submicrometer lateral resolution using focused ion beams. Analogous studies that involve depth profiling through molecular layers have been less successful. The incident ion beam usually destroys a fraction of the molecules and the remaining fragments build up at the surface, masking the desired signal. If these problems could be overcome, this capability would have major implications for a number of fields, including molecular electronics and the assay of molecular thin-film structures and biology where the three-dimensional mass spectra of single biological cells could be achieved.

There have been several notable examples where molecular depth profiling has been attempted with reasonable success. Several groups have reported that damage accumulation is reduced when using cluster beam sources.[1−6] The idea is that if the incident energy is deposited close to the surface and the yield, i.e., the number of molecules removed per impinging projectile ion, is high enough to prevent damage accumulation, intact molecules may be continuously desorbed from the sample. For example, Gillen and Roberson have found that the molecular ion intensity from a glutamate film remains constant after an initial decline when bombarded by 3-keV SF_5^+ ions at least up to a fluence of 10^{15} cm^{-2}.[7] More recently, similar observations have been reported with a C_8^- ion beam source using an amino acid thin film as a model.[8] Using massive, multiply charged clusters of glycerol molecules as projectiles, Cornett and co-workers[9] demonstrated that massive cluster impact produces stable secondary ion signals of large biological molecules desorbed from dried films on a metallic substrate even after prolonged exposure to the primary ion beam. This work was later followed by Todd et al.,[10] who showed that these projectiles may even be used to remove the damage previously generated by a different ion beam.

In this work, we report on the use of a buckminsterfullerene (C_{60}) cluster ion projectile combined with the use of water−ice as a matrix for target molecules. Recent experiments suggest that a C_{60}^+ ion beam is a candidate probe for molecular depth profiling experiments. This material has been developed as a valuable new addition to the repertoire of cluster beam sources, and the cluster

* Corresponding author. E-mail: wucher@uni-essen.de. Phone: +49 (201) 183 4141. Fax: +49 (201) 183 93 4141.

† University of Duisburg−Essen.

‡ The Pennsylvania State University.

(1) Hagenhoff, B.; Cobben, P. L.; Bendel, C.; Niehuis, E.; Benninghoven, A. In *Secondary Ion Mass Spectrometry (SIMS XI)*; Gillen, G., Lareau, R., Bennett, J., Stevie, F., Eds.; Wiley & Sons: Chichester, U.K., 1998; pp 585−588.

(2) van Stipdonk, M. J.; Harris, R. D.; Schweikert, E. A. In *Secondary Ion Mass Spectrometry (SIMS XI)*; Gillen, G., Lareau, R., Bennett, J., Stevie, F., Eds.; Wiley & Sons: Chichester, U.K., 1998; pp 877−882.

(3) Diehnelt, C. W.; van Stipdonk, M. J.; Harris, R. D.; Schweikert, E. A. In *Secondary Ion Mass Spectrometry (SIMS XI)*; Gillen, G., Lareau, R., Bennett, J., Stevie, F., Eds.; Wiley & Sons: Chichester, U.K., 1998; pp 593−596.

(4) Gillen, G.; Fahey, A. *Appl. Surf. Sci.* **2003**, *203−204*, 209−213.

(5) Wagner, M. S. *Anal. Chem.* **2004**, *76*, 1264−1272.

(6) Mahoney, C. M.; Roberson, S.; Gillen, G. *Anal. Chem.* **2004**, *76*, 3199−3207.

(7) Gillen, G.; Roberson, S. *Rapid Commun. Mass Spectrom.* **1998**, *12*, 1303−1312.

(8) Gillen, G. *Microbeam Analysis 2000*; pp 339−340 (Inst. Phys. Conf. Ser. 165).

(9) Cornett, D. S.; Lee, T. D.; Mahoney, J. F. *Rapid Commun. Mass Spectrom.* **1994**, *8*, 996−1000.

(10) McMahon, J. M.; Dookeran, N. N.; Todd, P. J. *J. Am. Soc. Mass Spectrom.* **1995**, *6*, 1047−1058.

10.1021/ac049641t CCC: $27.50
Published on Web 11/05/2004

has a size that is intermediate to the smaller and larger clusters noted above. The source has the special attributes that it operates in a very stable fashion for several hundred hours, is focusable to ~1 μm for imaging experiments, and produces molecular ion yields, i.e., numbers of intact molecular secondary ions desorbed per projectile impact, that are by orders of magnitude larger than found for atomic beam sources. For various thick organic films, C_{60}^+ bombardment has been reported to result in much lower damage cross sections and slower decays of molecular ion signals than atomic projectiles.[11,12] With this projectile, the yield of water molecules from an ice matrix is expected to be very high, given the low cohesive energy of this solid. Moreover, if molecular depth profiling protocols can be worked out for a variety of molecules dissolved in water, this would have major implications for the three-dimensional analysis of biomaterials prepared in their in vivo aqueous environment.

As a test case for such an analysis, we examine the bombardment of a frozen aqueous solution of histamine by 20-keV C_{60}^+ ions and compare the results to similar experiments using 15-keV Ga^+ ion bombardment. In general, the secondary-ion yield of histamine molecules is more than 2 orders of magnitude higher using the C_{60}^+ probe, although the qualitative features of the SIMS spectra, including those peaks arising from water clusters, are very similar. The histamine signal rapidly decays during bombardment with the atomic projectile but is observed to be restored to the initial value after exposure to C_{60}^+ ion bombardment.

With a quartz crystal microbalance (QCM), we find there are ~2400 ice molecules removed for each cluster ion impact, indicating that the rate of removal of material may be faster than the damage accumulation. We show that histamine mass spectra may be acquired under high-dose conditions without significant complication from chemical damage. The fluence dependence of the measured signals suggests that there is an excess of histamine molecules within 5 nm of the ice surface, which may arise from the specific adsorption of histamine to the liquid−vapor interface or thermal desorption of ice molecules in the vacuum chamber. Moreover, the C_{60}^+ probe is shown to be effective at removing matrix overlayers, which may otherwise mask the mass spectral information associated with the target molecule. Finally, the data suggest it will be feasible to erode the ice using the cluster ion probe, while using the Ga^+ ion probe to collect high-resolution molecule-specific images as a function of depth.

EXPERIMENTAL SECTION

Experiments were performed in an ultrahigh vacuum time-of-flight mass spectrometer (TOF-MS) described elsewhere.[13] Briefly, secondary ions released from the sample surface by ion bombardment are accelerated by a pulsed extraction field and mass selected according to their flight time by a reflecting mirror analyzer. Neutral molecules are detected by photoionization with a femtosecond-pulsed laser focused a few millimeters above the sample surface.

Ion Sources. To initiate molecular desorption, the system is equipped with two primary ion sources. The first one is a standard liquid metal ion source (Ionoptika Ltd., Southhampton, U.K.), which is operated under conditions producing a finely focused beam of 15-keV Ga^+ ions with a diameter of ~0.5 μm at a beam current of several nanoamperes. The second source is a newly developed fullerene ion source that has been designed to produce C_{60} cluster ions.[11,12] The operation principle is based upon thermal evaporation of neutral C_{60} clusters from a heated reservoir containing C_{60} powder. The vapor is then ionized by electron impact. In general, this source delivers a relatively pure beam of C_{60} ions with a distribution of singly and doubly charged species. Under normal operating conditions, these two charge states may be separated by means of a flight time filter employing two pairs of pulsing plates located in the beam path. This scheme was not employed in the present work since it only permits the production of ion pulses with duration below 100 ns. Since an objective of this study is to accumulate relatively large primary ion fluence, it was necessary to employ a dc ion beam. The C_{60} ion source was therefore operated with the relatively low electron impact energy of 30 eV, whereby the multiply charged ions are largely suppressed due to their higher ionization potential. Under these conditions, the generated beam of C_{60}^+ ions exhibits a total current of ~1 nA into a spot of ~20-μm diameter at the sample surface.

The two ion beams impinge onto the investigated surface under an impact angle of ~50° with respect to the surface normal. To allow the mass spectral analysis of a surface region using both Ga^+ and C_{60}^+ projectiles, it is necessary to carefully align both ion beams to hit the same spot at the sample surface. Moreover, the exact determination of ion fluence requires good calibration of both the raster area and the beam diameter. All three tasks were accomplished by means of ion-induced electron images of a TEM copper grid. To expose the same square raster area on the surface, the different impact azimuth of both ion beams was compensated by electronic rotation of the raster pattern. The raster area was calibrated using the known mesh width of the grid. To arrive at the true irradiated surface area—which is important in order to calculate the ion fluence—the beam diameter must be added to the dimension of the raster area. The effective beam diameter was therefore determined from line scans across a grid bar using the 90−10% transition width.

Laser Photoionization. Ionization of sputtered neutral molecules (postionization) was performed using a short-pulse laser described in detail elsewhere.[14] The system delivers pulses of ~1 mJ and 120-fs duration at a wavelength of 800 nm and a repetition rate of 1 kHz. The beam is focused into the vacuum chamber by a 250-mm-focal length quartz lens, which was retracted in such a way that the beam diameter in the postionization region above the surface is 150 μm.

Timing. A few words are in order to describe the relative timing of the various pulses involved in the experiment. During spectrum acquisition, the primary ion beam is operated in a pulsed mode with a pulse duration of ~50 ns. Since the beam alignment procedure described above ultimately requires the sample surface to be kept at ground potential during the ion bombardment, the electrostatic field extracting the sputtered particles into the mass

(11) Weibel, D.; Wong, S.; Lockyer, N.; Blenkinsopp, P.; Hill, R.; Vickerman, J. C. *Anal. Chem.* **2003**, *75*, 1754−1764.
(12) Wong, S. C.; Hill, R.; Blenkinsopp, P.; Lockyer, N. P.; Weibel, D. E.; Vickerman, J. C. *Appl. Surf. Sci.* **2003**, *203*, 219−222.
(13) Braun, R. M.; Blenkinsopp, P.; Mullock, S. J.; Corlett, C.; Willey, K. F.; Vickerman, J. C.; Winograd, N. *Rapid Commun. Mass Spectrom.* **1998**, *12*, 1246.
(14) Willey, K. F.; Brummel, C. L.; Winograd, N. *Chem. Phys. Lett.* **1997**, *267*, 359−364.

spectrometer was switched on shortly (~50 ns) after the end of the projectile pulse by applying a potential of +2500 V to the sample stage. Care was taken to compensate for the different arrival times of Ga^+ and C_{60}^+ ions at the sample surface, thus keeping the time delay between projectile impact and extraction pulse constant upon switching between both guns. For laser postionization experiments, the ionization laser pulse was fired 300 ns after the stage potential was switched on. Due to the short primary ion pulses used, this time delay is necessary to allow sputtered neutral particles to travel into the ionization volume. In connection with the laser−surface distance of ~1 mm, the selected emission velocity of ~3 km/s roughly corresponds to the maximum of the emission velocity distribution of sputtered particles. The stage potential was kept high for ~2 μs and then switched back to ground potential in order to permit the compensation of the primary ion charge using low-energy electrons.

Charge Compensation. Although the investigated ice samples are electrical insulators, charge compensation is generally not necessary with the C_{60}^+ ion beam. This phenomenon has been observed for other samples as well and is attributed to the high total yields of positive secondary ions under C_{60}^+ ion bombardment. In connection with the Ga^+ ion beam, on the other hand, charge compensation is needed in order to acquire meaningful spectra. This is accomplished with a low energy electron gun delivering ~1 μA beam current into a spot of ~1-mm diameter at an electron energy of 20 eV. During spectrum acquisition, the electron beam is operated in a pulsed mode with a pulse of 50-μs duration that is fired ~50 μs after the termination of the ion extraction pulse, thus hitting the surface while the sample is at ground potential. During the dc bombardment cycles employed to accumulate large primary ion fluence, the sample was permanently kept at ground potential and the electron beam was switched to dc mode as well.

Sample Preparation. The samples were prepared by depositing ~2 μL of an aqueous solution of histamine (1.6 mg/mL) onto a silver substrate that had been etched in HNO_3 and thoroughly rinsed in deionized water and methanol. The sample was then frozen by slowly immersing the Cu sample mount block into liquid nitrogen. This method, referred to as "slow freeze", produces relatively thin and homogeneous ice films with visible crystallites of several hundred micrometers diameter. This sample was used in all experiments unless stated otherwise in the text. In some cases, a different protocol was employed by cooling the Cu block to liquid nitrogen temperature prior to applying the sample solution. This "fast-freeze" procedure leads to a relatively thick droplet of ice at the center of the substrate. The sample was introduced into the vacuum chamber by means of a fast entry lock and loaded onto a liquid nitrogen-cooled sample stage that was kept at a temperature of ~100 K. Visual inspection using a zoom microscope ensured that the ice film did not melt during the relatively short transfer time of typically 30 s.

RESULTS AND DISCUSSION

The central focus of this work is to examine the desorption behavior of histamine molecules from an ice matrix using the C_{60}^+ ion beam as an excitation source. To determine this behavior, we first examine the mass spectra of ice samples bombarded with either Ga^+ or C_{60}^+ ions in the traditional low-dose mode to minimize any effects of molecular decomposition. These spectra are then compared to those obtained from an ice surface that has been bombarded with a high dose of either C_{60}^+ or Ga^+ ions to determine whether this bombardment reduces the molecular information present in the spectra. A similar strategy then leads to actual depth profiling experiments with an ion fluence of up to 5×10^{14} cm^{-2}. Finally, we determine the total sputtering yield using a quartz crystal microbalance in order to estimate the actually eroded depth.

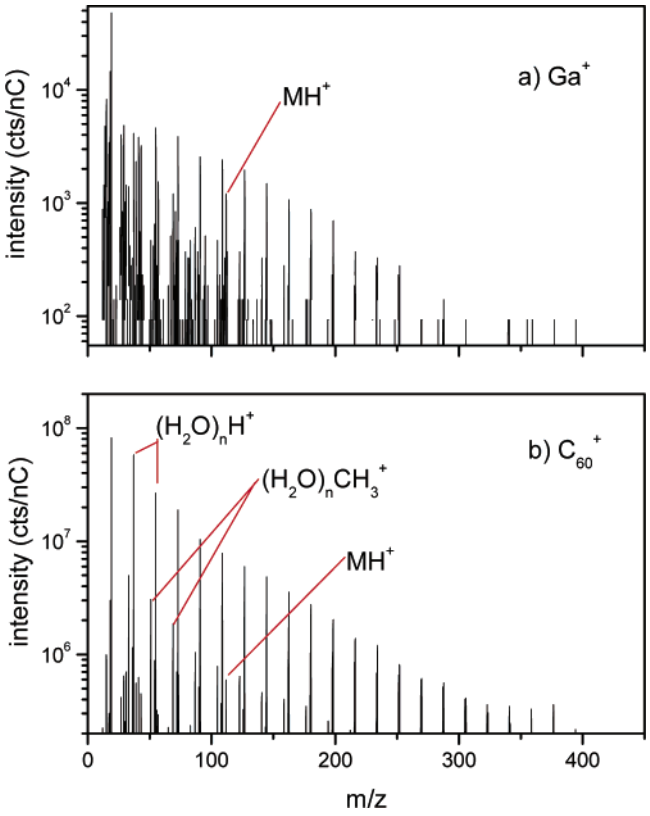

Figure 1. TOF-mass spectrum of ion beam-desorbed secondary ions measured on a freshly introduced frozen histamine/ice sample under bombardment (a) with 15-keV Ga^+ and (b) 20-keV C_{60}^+ ions.

Mass Spectra. The TOF-SIMS spectra measured on a freshly prepared histamine/ice sample immediately after introduction into the vacuum system are shown in Figure 1. The spectra were acquired using a total primary ion fluence of ~10^{10} cm^{-2}. The spectra, whether acquired with Ga^+ ions or C_{60}^+ ions, show a progression of $(H_2O)_nH^+$ cluster ions that closely resembles the TOF-SIMS spectrum of pure ice. In addition, the spectrum taken under C_{60}^+ ion bombardment exhibits a distinguished second progression of $(H_2O)_nCH_3^+$ cluster ions. This finding is consistent with the notion that the C_{60} molecule is obliterated upon impact with the ice and that free carbon atoms are available to form stable C-containing clusters via a recombination mechanism. In addition to these peaks, the spectrum produced by C_{60}^+ ions is remarkably pure. The spectrum resulting from Ga^+ ion bombardment shows the same progression of clusters but, in addition, contains a number of unspecific hydrocarbon peaks at low mass. Both spectra show a clearly discernible molecular ion signal of histamine at mass 112 Da $[(M + H)^+]$ as well as signals of characteristic fragments at masses 95 $[(M - NH_2)^+]$ and 83−81 Da $[(M - CH_{0-2}NH_2)^+]$. Other striking observations include the following:

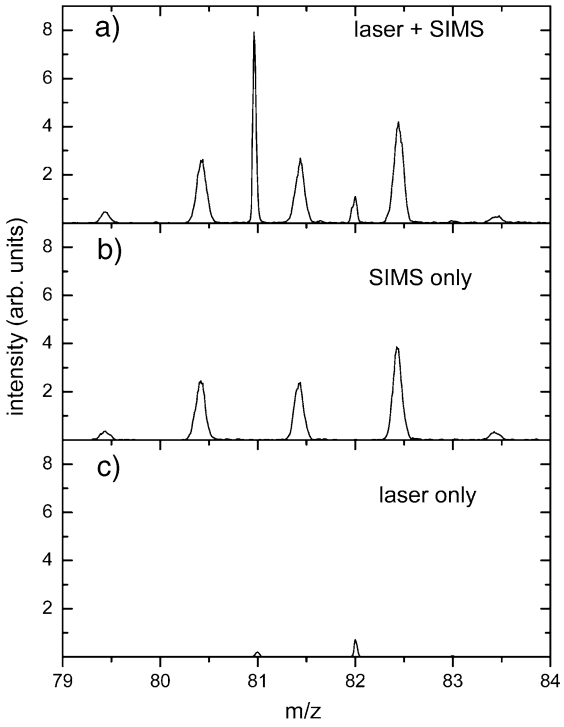

Figure 2. TOF-mass spectra of secondary ions and neutrals desorbed from a freshly introduced frozen histamine/ice sample measured with (a) 800-nm laser postionization laser, (b) without postionization laser, and (c) with postionization laser alone (no ion bombardment). For the ion beam desorption experiments, the sample was bombarded with 20-keV C_{60}^+ ions. For clarity, only the interesting region around the molecular histamine fragments is shown.

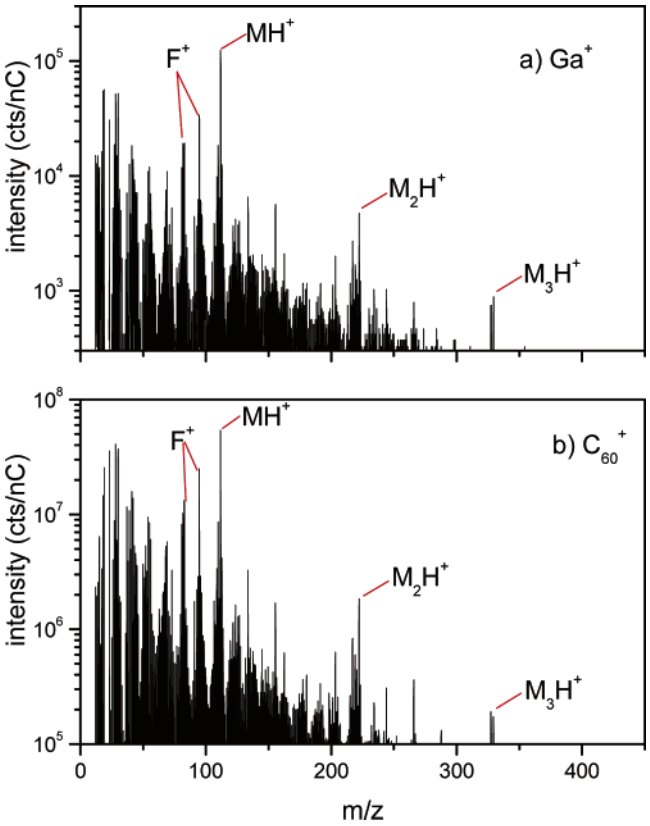

Figure 3. TOF-mass spectrum of ion beam-desorbed secondary ions measured on a frozen histamine/ice sample after prebombardment with 20-keV C_{60}^+ ions with a total fluence of ~10^{13} cm^{-2}.

(i) The signals produced by C_{60}^+ ion bombardment are much higher than those produced under Ga^+ ion bombardment (note that the spectra have been normalized to the dc current of the respective primary ion source and are reported in counts per nanocoulomb primary ion fluence). (ii) Even though the histamine-related molecular ion signals seem to be minority peaks in the total C_{60} spectrum, their absolute magnitude is several orders of magnitude larger than those visible in the spectrum recorded with Ga^+ ions.

Laser photoionization employed to detect desorbed neutral histamine molecules yielded only negligible signal at 111 (M^0) and 95 Da but a pronounced molecular fragment signal at 81 Da. To allow a clear discrimination of postionized neutral species from secondary ions, the relative timing of the primary ion pulse, the extraction pulse, and the laser pulse was chosen to produce different apparent flight times of the secondary ion and neutral flux. An example of such a measurement is shown in Figure 2. The upper panel (a) depicts a convolution of the ion and neutral spectrum. The middle panel (b) shows the SIMS spectrum measured without the postionization laser, which shows essentially the peaks arising from the fragments at 81, 82, and 83 Da. Note that the apparent mass of these peaks is shifted by a fraction of a mass unit due to the flight time separation mentioned above. The lower panel (c) depicts the residual gas spectrum measured with the postionization laser alone, i.e., with the primary ion beam switched off. It is evident that the residual gas signal is negligible at 81 Da and that the secondary ion and secondary neutral spectra are clearly separated.

The spectra depicted in Figure 1 represent the information that can be obtained in a static SIMS experiment. To investigate the possible influence of surface contamination overlayers or determine a possible depth distribution of the molecule, we now go beyond the static limit and erode the surface by bombarding with a dc ion beam. This type of experiment is illustrated in Figure 3, where spectra taken with Ga^+ ions and C_{60}^+ ions are shown after irradiating the surface with C_{60}^+ ions to a total fluence of 3 × 10^{13} cm^{-2}. To avoid crater edge effects, the raster area during this prebombardment was chosen to be larger (800 × 800 μm^2) than that used during spectral acquisition (500 × 500 μm^2). It is seen that both spectra have completely changed and are now clearly dominated by the histamine molecular ion signals. The cluster ion bombardment therefore not only preserves the molecular information but *enhances* these signals by ~2 orders of magnitude, demonstrating that the surface can be sputter-cleaned and eroded without destroying the molecular information. Note that the magnitude of the histamine signal increase is about the same in the spectra taken under C_{60}^+ and Ga^+ ion bombardment. At the same time, the signals related to water−ice have decreased significantly, indicating that histamine may be enriched at the ice−vacuum interface.

If the surface is further eroded by bombardment to a higher C_{60}^+ ion fluence, the molecular signal is found to decrease again, until in the limit of high fluence, a steady state appears to be reached. An example of the spectra measured after a C_{60}^+ fluence of 3 × 10^{14} cm^{-2} is shown in Figure 4. It is seen that in the C_{60}^+ spectrum the molecular signals have decreased by ~1 order of magnitude, while the water−ice-related signals are found to

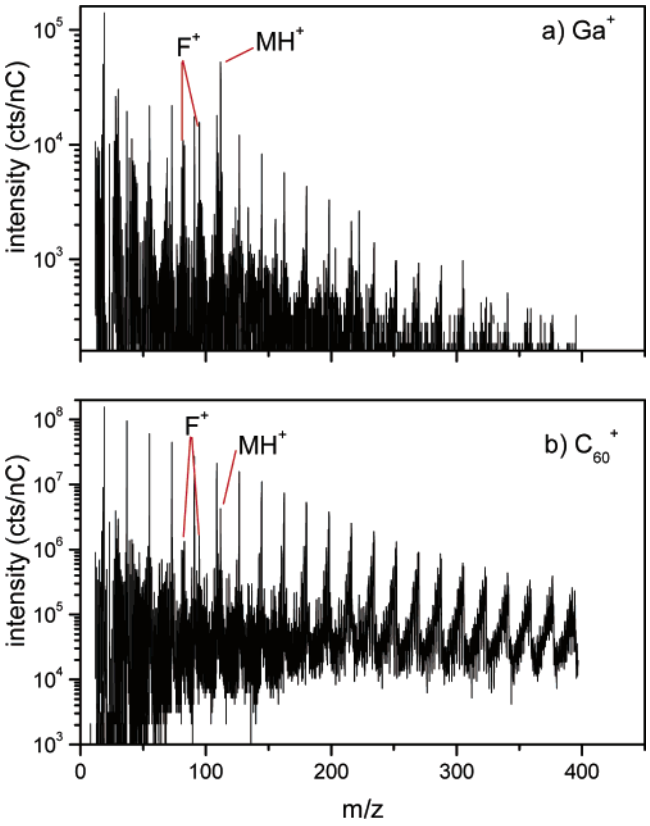

Figure 4. TOF-mass spectrum of ion beam-desorbed secondary ions measured on a frozen histamine/ice sample after prebombardment with 20-keV C_{60}^+ ions with a total fluence of ~10^{14} cm^{-2} (steady state).

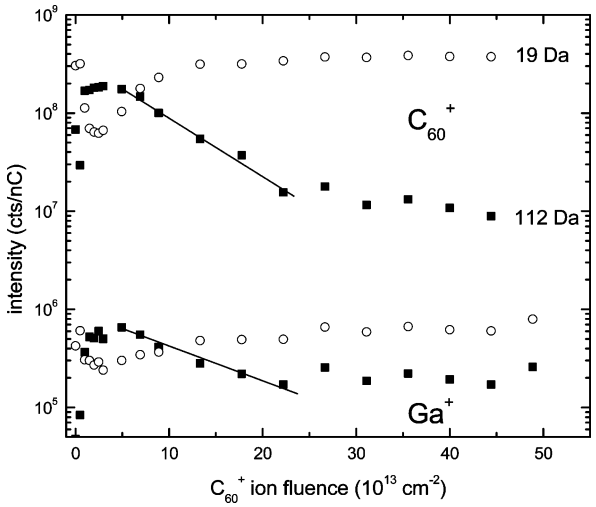

Figure 5. Dependence of signals of ion beam-desorbed histamine molecular ions (112 Da) and ice matrix-specific $(H_2O)H^+$ ions (19 Da) on the total fluence of C_{60}^+ ions used to prebombard the surface. Upper track, data taken under 20-keV C_{60}^+ ion bombardment; lower track, data taken under 15-keV Ga^+ ion bombardment.

increase back to their original level. The Ga^+ spectrum, however, behaves differently. Here, the reduction of the molecular signal is much less pronounced, and the steady-state signals are almost comparable to those measured with C_{60}^+ projectiles. In fact, the Ga^+ spectrum appears to be still dominated by the histamine signal. In any case, the data clearly demonstrate that Ga^+ projectiles may be employed just as well as C_{60}^+ projectiles in order to acquire the molecular signal in a sputter depth profile, provided the surface erosion is performed with the C_{60}^+ cluster ion beam.

Depth Profiles. To assess the ion beam-induced damage and evaluate molecular depth profiling capabilities, it is essential to investigate the dependence of the measured signal on the fluence of the projectile ions employed for surface erosion. This dependence for selected peaks of the data presented in the previous subsection is illustrated in Figure 5. More specifically, the measured signals at 112 (histamine) and 19 Da (ice) were integrated over the respective peaks and plotted against the total accumulated C_{60}^+ ion dose. To allow a quantitative comparison of data taken with Ga^+ or C_{60}^+ projectiles, the signals were normalized to both the number of shots used to accumulate the spectrum and the primary ion current. It is seen again that the signal produced by 15-keV Ga^+ ion bombardment is by more than 2 orders of magnitude lower than that generated by 20-keV C_{60}^+ projectiles. The variation of both signals with increasing C_{60}^+ prebombardment fluence, however, is largely the same: After a steep initial rise, the histamine signal is found to remain practically constant in an interval of several 10^{13} cm^{-2}, until at larger fluences it starts to decrease again. This maximum, accompanied by a dip of the ice signal, indicates that histamine is enriched at the surface.

Above a fluence of ~6×10^{13} cm^{-2}, the histamine signal is found to decrease exponentially until the fluence exceeds 10^{14} cm^{-2}, where a steady state appears to be reached. At the same time, the ice-related signal recovers to its initial value and remains constant thereafter. This observation is strong evidence that the total sputter yield remains constant. Note that the magnitude of signal reduction is different for the spectra taken under C_{60}^+ and Ga^+ bombardment. This finding may in principle arise from a preferential sputtering effect typical for dual-beam depth profiling: Since the surface is heavily prebombarded with C_{60}^+, the spectrum taken under C_{60}^+ bombardment reflects steady-state sputtering conditions where the flux of desorbed histamine and ice must match the bulk histamine concentration in the ice sample. The (static) spectrum taken under Ga^+ bombardment, on the other hand, does not fulfill this condition. Therefore, if the sputtering efficiency of histamine relative to that of ice is larger for 15-keV Ga^+ impact than under 20-keV C_{60}^+ impact, the relative contribution of histamine-related signals in the Ga^+ spectrum will be larger, as observed in Figure 5. The apparent difference in the slope of the exponential signal decay is due to the different asymptotic signal levels at high fluence. Subtracting this constant background yields in both cases a similar decay constant σ around 2×10^{14} cm^2.

The fluence dependence of various histamine-derived fragment ions and the molecular ion itself (as displayed in Figure 5) are shown in Figure 6. To cover a wide range of fragmentation products, the selection includes the molecule-specific fragments at masses of 95, 83, 82, and 81 Da as well as an unspecific fragment at mass 28 Da. All fragment ion signals follow the same trend as the intact molecular ion. This finding is important, since it indicates that the observed signal decay is not induced by the accumulation of ion bombardment-induced chemical damage. Several other pieces of data supporting this hypothesis are given in the subsections below.

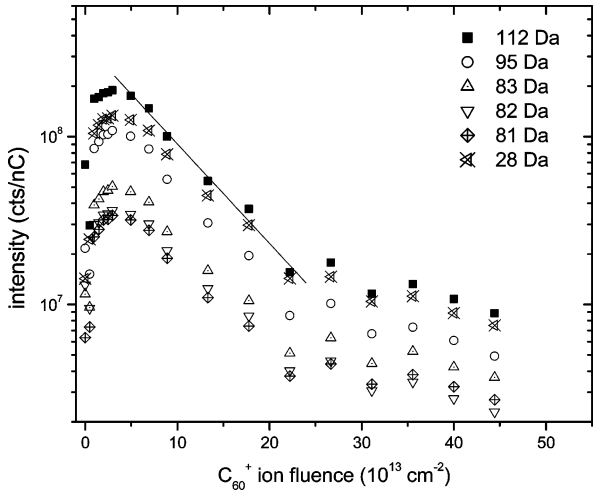

Figure 6. Signal of ion beam-desorbed histamine molecular ions (112 Da) along with characteristic (95, 83, 82, and 81 Da) and noncharacteristic (28 Da) fragment ions measured under bombardment with C_{60}^+ ions as a function of the total C_{60}^+ prebombardment ion fluence.

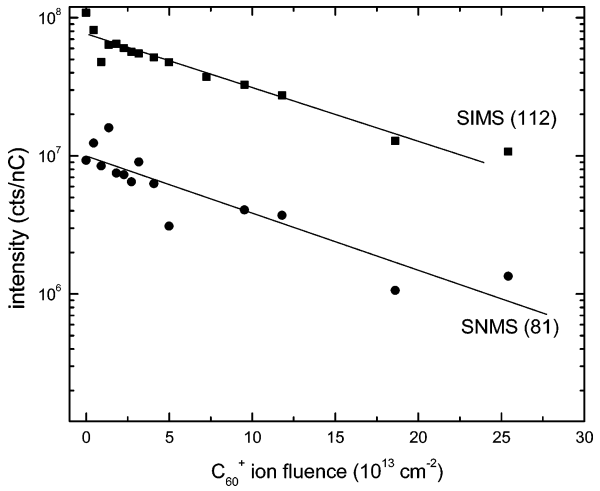

Figure 7. Dependence of signals of ion beam-desorbed histamine molecular ions (112 Da) and postionized neutral histamine fragments (81 Da) on the total fluence of C_{60}^+ ions used to prebombard the surface. Spectrum acquisition was performed under 20-keV C_{60}^+ ion bombardment.

It should be noted that the same behavior as depicted in Figure 5 is observed for postionized neutral molecular fragments. This finding is also important since it indicates that the observed decay of the secondary ion signals is not caused by (concentration-dependent) variations of the ionization probability of the desorbed species. As an example, the fluence dependence of the 81-Da neutral fragment signal along with that of the 112-Da parent secondary ion is shown in Figure 7. Note that the signal variation is very well reproduced, even though this experiment was performed on a different day using a different sample and different raster areas, respectively.

Ga^+ Bombardment. It is essential to determine whether the retention of molecular information under C_{60}^+ bombardment is associated with the cluster nature of the projectile. To investigate this point, we switch between using Ga^+ ions and C_{60}^+ ions to prebombard and erode the surface. As shown in Figure 8, TOF-SIMS spectra were recorded under 20-keV C_{60}^+ and 15-keV Ga^+

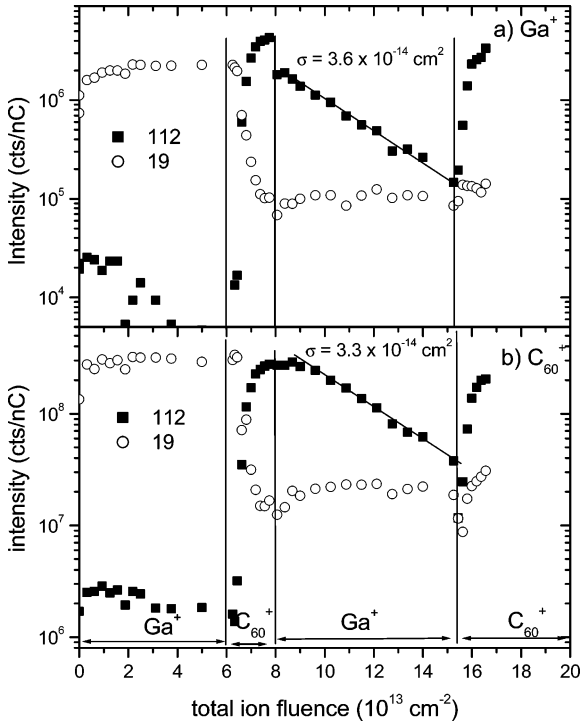

Figure 8. Signal of ion beam-desorbed histamine molecular ions (112 Da) and ice matrix-specific $(H_2O)H^+$ ions (19 Da) measured under bombardment with (a) C_{60}^+ and (b) Ga^+ ions as a function of the total prebombardment ion fluence. Prebombardment was performed alternatively with 15-keV Ga^+ and 20-keV C_{60}^+ ions as indicated in the figure.

bombardment, respectively, and the integrated signals of the histamine molecular ion and the water molecule are plotted against the total prebombardment ion fluence.

On the freshly prepared surface, a pure spectrum of water–ice is found prior to prebombardment that contains a very weak histamine signal. This situation remains unchanged even if the surface is bombarded with Ga^+ ions up to a total fluence of $\sim 6 \times 10^{13}$ cm^{-2}. Apparently, the Ga^+ bombardment is not capable of uncovering the histamine signal. If the prebombardment is switched to the C_{60}^+ ion beam, on the other hand, the signal immediately rises to a maximum value, which is reached at a C_{60}^+ fluence of $\sim 10^{13}$ cm^{-2}. At the same time, the ice signal is depleted just as observed before. Switching back to Ga^+ bombardment, the molecular histamine signal decreases exponentially with increasing fluence, while the ice signal remains constant. Evidently, the Ga^+ beam induces accumulating damage with increasing fluence, leading to a disappearance cross section of 3×10^{-14} cm^2. By switching the sputtering beam back to C_{60}^+, the histamine signal is rapidly restored. Clearly, the damage induced by the Ga^+ beam is removed under C_{60}^+ bombardment. This observation is consistent with the earlier findings of Todd et al.,[10] who demonstrated the use of massive cluster impact to remove atomic ion-produced damage from organic surfaces.

Sample Preparation Issues. To examine the influence of the applied sample preparation method, a different preparation technique was tested, where the sample block was now cooled to liquid nitrogen temperature *prior* to deposition of the sample solution. In this case, it is not possible to achieve a thin ice layer. Instead, the deposited solution freezes as a relatively thick droplet on the

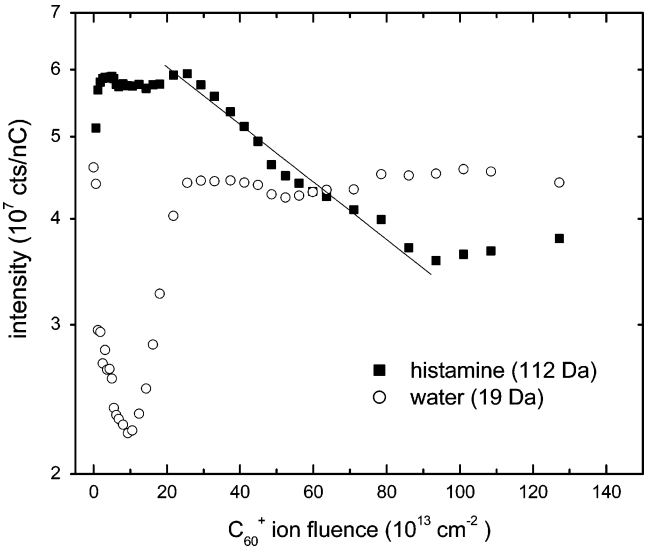

Figure 9. Signal of ion beam-desorbed histamine molecular ions (112 Da) and ice matrix-specific $(H_2O)H^+$ ions (19 Da) as a function of the total prebombardment ion fluence measured on a histamine/ice sample prepared by the fast-freeze technique. Both sputter erosion and data acquisition were performed using 20-keV C_{60}^+ ions.

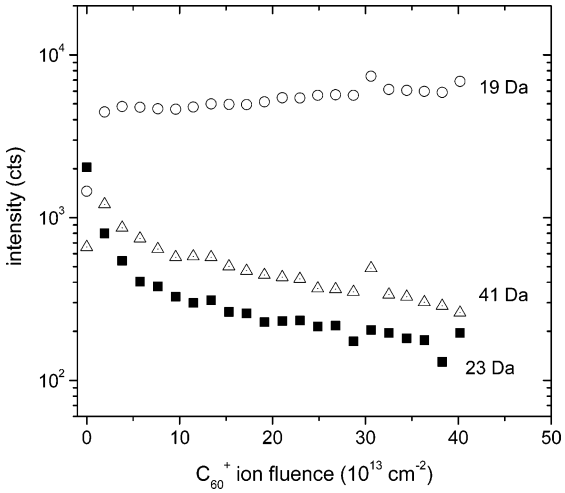

Figure 10. Signal of ion beam-desorbed Na^+ ions (23 Da), (H_2O)-H^+ ions (19 Da) and $(H_2O)Na^+$ ions (41 Da) on a NaCl/ice sample prepared by freezing an 18 mM solution of NaCl in water. Both sputter erosion and data acquisition were performed using 20-keV C_{60}^+ ions.

substrate surface. A depth profile that has been measured on such a sample is illustrated in Figure 9. It is seen that the histamine signal rises sharply at the surface and remains constant over a much larger fluence range than observed before. The dip of the ice signal, although still present, is less pronounced than seen in Figure 5, and the magnitude of the signal decrease between the maximum and the steady state at high fluences is reduced to a factor of ~1.5.

The apparent influence of the sample preparation method suggests that the observed signal variations are caused by actual concentration gradients in the sample rather than by chemical damage accumulation. For the types of samples investigated here, such gradients may originate from a wide range of possible sources. From a fundamental perspective, when a thin layer of liquid solution is deposited onto a metal substrate, the histamine concentration need not necessarily be homogeneously distributed through the film. In fact, a surface enrichment of analyte species in solutions was demonstrated nearly 75 years ago in elegant microtome experiments and was attributed to enhanced adsorption at the liquid−gas interface.[16] From a sample preparation perspective, the physical act of cooling the thin film may cause various perturbations. Using the protocol described in the Experimental Section, freezing proceeds from the bottom to top of the film. Evaporation during the cooling process may therefore lead to further histamine enrichment at the surface. After cooling, the surface begins to adsorb and condense water from the atmosphere. During the time needed to introduce the sample into the vacuum system, a relatively pure ice film will therefore develop on top of the originally prepared sample. As a consequence of these processes, the sample actually studied in the depth profile analysis may in principle contain a buried, histamine-enriched subsurface layer. To examine that hypothesis, the depth profiling experiment was performed on a test ice sample prepared from an 18 mM acqueous solution of sodium chloride without the presence of histamine. The resulting C_{60}^+ fluence dependences of the Na^+ (23 Da), the $(H_2O)H^+$ (19 Da), and the $(H_2O)Na^+$ signals are shown in Figure 10. While the ice signal exhibits an initial increase and then remains constant, the Na^+ signal is largest at the surface and strongly decreases with increasing fluence. At the same time, the $(H_2O)Na^+$ signal exhibits a maximum value since the efficient production of this secondary ion requires both the Na and the H_2O surface concentrations to be large. It is clear that the signal variations observed in this case are not related to chemical damage accumulation. Nevertheless, the Na^+ signal is found to decay in a fashion quite similar to that observed for the histamine-related signals shown in Figures 5−9. In this case, the signal must represent a true concentration gradient, indicating that Na is enriched in a surface layer of thickness comparable to those observed in the histamine experiments. Although this observation does not constitute a proof of our postulate of a histamine-enriched surface layer, it shows that such layers may feasibly form at some stage during the sample preparation technique employed here.

Sputtering Yield. It has been discussed in the literature[6−10] that chemical damage accumulation in molecular sputter depth profiling is reduced by cluster ion beams due to the fact that the sputtering yields induced by such projectiles are significantly larger than those obtained under atomic projectile impact. As a consequence, the damage can be removed as fast as it is produced, leading to a steady-state molecular signal at high ion fluences. To assess this possibility for the conditions of the present work, the amount of material removed from the ice sample was determined using a QCM. For that purpose, the sample holder was modified to accommodate a 6-MHz quartz crystal, and an ice sample was prepared on that crystal instead of the silver substrate. Unfortunately, pure water does not wet the gold contact layer deposited on the quartz crystal. To obtain a fairly homogeneous ice layer, a mixture of 30% ethanol and 70% water was deposited and frozen instead. The QCM measurement procedure was tested at room temperature on the bare gold contact layer, where the

(15) Cliff, B.; Lockyer, N. P.; Corlett, C.; Vickerman, J. C. *Appl. Surf. Sci.* **2003**, *203*, 730−733.
(16) McBain, J. W.; DuBois, R. *J. Am. Chem. Soc.* **1929**, *51*, 3534−3549.

controller depicted a mass removal rate of $\sim 1.0 \times 10^{-8}$ g/(cm^2 s) upon bombardment with a total current of 1.7 nA of C_{60}^+ ions. The same measurement was repeated with the sample stage cooled to 100 K, where the resonance frequency exhibited some thermal drift and the reading of the deposition rate was not as stable as at room temperature. However, it was still possible to obtain a statistically significant reading of the same magnitude on the gold layer. When the ice layer was prepared on the crystal and bombarded, a mass removal rate of 4.6×10^{-8} g/(cm^2 s) was measured. To determine absolute values of mass removed per unit time, the measured removal rate must be multiplied by the active area A of the quartz surface, which was measured to be $\sim$2 mm in diameter. [19] The sputtering yield is then determined by

$$Y_{\text{tot}} = \frac{rAN_{\text{A}}e}{MI_{\text{p}}} \quad (1)$$

with r being the measured mass removal rate, N_{A} Avogadro's constant, e the elementary charge, M the atomic or molecular weight of the target material, and I_{p} the primary ion current. For the gold surface, the resulting sputtering yield is $Y_{\text{tot}} \sim 90$ atoms per 20-keV C_{60}^+ ion.

Neither experimental nor theoretical sputtering yield data exist for C_{60}^+ impact onto a gold target that could be used for direct comparison. Molecular dynamics computer simulations of 15-keV C_{60} bombardment of a single crystal (111) silver surface, on the other hand, have revealed a yield of $\sim$220 sputtered Ag atoms per C_{60} projectile for a 45° impact angle.[20] In view of the fact that the sublimation energy of gold (3.4 eV) is slightly larger than that of silver (3.0 eV), gold is expected to exhibit a lower sputtering yield. Hence, the value determined here appears reasonable.

For the ice target, assuming stoichiometric sputtering and using $M = (0.3 \times 46 + 0.7 \times 18)$ g, we obtain a sputtering yield of $Y_{\text{tot}} \sim 3100$ ice molecules per C_{60}^+ ion of 20 keV. This estimate presumably overestimates the actual yield of pure water−ice since the cohesive energy is reduced by the ethanol admixture. To estimate the magnitude of this effect, we adopt a common protocol[21,22] to calculate the cohesive energy density of the liquid solution as a linear superposition of the respective values for water (2294 MPa) and ethanol (676 MPa) and assume that the cohesive energy of the frozen sample changes accordingly. The resulting cohesive energy of the admixed ice sample is reduced by $\sim$20% with respect to that of pure water−ice. Assuming the generally accepted inverse proportionality between sputter yield and cohesive energy, the sputter yield of pure water−ice under the C_{60}^+ bombardment conditions employed here is $\sim$2400 molecules/ion.

In comparison with published data on sputtering yields of water−ice, this value appears surprisingly large. For instance, Christiansen et al.[23] measured yield values near 20 molecules/ion under Ar^+ bombardment with kinetic energies between 10 and 30 keV. The yield under 20-keV Ar^+ ion impact has been measured by Baragiola et al.[24] as 25 molecules/ion, an interpolation of their data for Xe^+ impact results in a value of $\sim$55 molecules/ion at 20 keV. Probably the largest absolute yield value reported so far is 90 molecules/ion for 30-keV O_2^+ bombardment.[24] Clearly, the impact of C_{60} clusters is more efficient in producing sputtering action at the ice surface than any atomic projectile of comparable energy.

Due to a residual thermal drift, it was not possible to obtain a statistically meaningful mass removal rate reading on the ice sample under 15-keV Ga^+ bombardment. From signal-to-noise ratio considerations, the sputter yield under Ga^+ impact must be at least 10-fold lower than that under C_{60}^+ impact. Extrapolating from literature data,[23,24] a sputter yield of $\sim$50 molecules/ion under 15-keV Ga^+ impact is expected. The resulting 50-fold difference between Ga and C_{60} projectiles is a factor of 2−3 lower than the observed enhancement of the molecular histamine secondary ion signal (cf. Figure 5). This finding indicates that the cluster impact may be more efficient in producing molecular ions from a given eroded sample volume. However, the ambiguity involved in the data reduction process outlined above appears too large to make a more rigid assessment at this point.

If the measured sputtering yield is combined with the density of water−ice ($\sim$0.9 g/cm^3), a C_{60}^+ ion fluence of 1×10^{13} cm^{-2} is estimated to lead to the removal of a surface layer of $\sim$8-nm thickness. The total dose applied in Figure 5 therefore corresponds to the removal of $\sim$0.5 μm of material from the surface.

CONCLUSION

The data presented here indicate that the use of C_{60} cluster projectiles provides a valuable tool for sputter depth profiling of molecular analytes in frozen aqueous matrixes. In particular, a molecular secondary ion yield enhancement by more than 2 orders of magnitude is found in comparison to atomic Ga^+ projectiles of comparable impact energy. It is shown that this signal increase is predominantly caused by a correspondingly large enhancement of the total sputter yield. At the same time, decay constants measured under conditions of high projectile ion fluences are *not* enhanced but tend to be even smaller than those observed under atomic ion bombardment. As a consequence, the damage induced by the projectile impact appears to be removed fast enough to prevent significant accumulation. In contrast to attempts where atomic projectiles are used for sputter removal, it is found that the sample can be eroded up to micrometer scale depths without destruction of the molecular signal. This finding is in accord with data obtained by Weibel and co-workers,[11] who demonstrated low-damage sputter depth profile analysis of various thick organic layers on silicon using the same C_{60}^+ ion source as employed here. The results obtained in this work follow the same trend that has been observed by other groups using different polyatomic projectiles. In particular, the significant improvement with increasing projectile cluster size that has been discovered by Gillen and co-workers[4] using carbon cluster projectile ions C_1−C_{10} seems to

(17) Gillen, G.; Simons, D. S.; Williams, P. *Anal. Chem.* **1990**, *62*, 2122−2130.
(18) Westley, M. S.; Baratta, G. A.; Baragiola, R. A. *J. Chem. Phys.* **1998**, *108*, 3321−3326.
(19) C. Szakal, A. Wucher, and N. Winograd, to be published.
(20) Postawa, Z.; Czerwinsky, B.; Szewczyk, M.; Smiley, E. J.; Winograd, N.; Garrison, B. J. *J. Phys. Chem. B* **2004**, *108*, 7831−7838.
(21) Van Uden, N. W. A.; Hubel, H.; Faux, D. A.; Dunstan, D. J.; Royer, C. A. *High-Pressure Res.* **2003**, *23*, 205−209.
(22) Van Uden, N. W. A.; Hubel, H.; Faux, D. A.; Tanczos, A. C.; Howlin, B.; Dunstan, D. J. *J. Phys.-Condens. Mater.* **2003**, *15*, 1577−1584.
(23) Christiansen, J. W.; Carpini, D. D.; Tsong, I. S. T. *Nucl. Instrum. Methods B* **1986**, *15*, 218−221.
(24) Baragiola, R. A.; Vidal, R. A.; Svendsen, W.; Schou, J.; Shi, M.; Bahr, D. A.; Atteberrry, C. L. *Nucl. Instrum. Methods B* **2003**, *209*, 294−303.

be continued up to C_{60}. Although similar trends have been found for reactive cluster projectiles such as SF_5^+ as well,[26] it is not entirely clear if the underlying mechanism is the same. For instance, Fuoco et al. have shown that the large improvement over Ar^+ projectiles that has been found for PMMA layers is *not* due to a significantly increased sputtering yield.[27] Similar to the effect found for sputtered metal clusters,[28] the ionization mechanism leading to the formation of sputtered molecular secondary ions must also be enhanced in that case.

The histamine molecule investigated here represents an important prototypical biomolecule. In view of the employed detection method, the basic nature of this species might be useful since the molecule can easily accept a proton from the aqueous environment in order to form a positive ion in the course of the desorption process. To explore the role of acidity/basicity in these experiments in more detail, it is interesting to extend the work to other molecules such as amino acids. Corresponding experiments are currently under way in our laboratory.

The sputter depth profiling capability of ice matrixes has important implications for bioimaging applications. As an example, the detection of relevant molecules in biological cells and the analysis of their spatial distribution seems now feasible using conceptually simple sputter depth profiling techniques. Without the sputter sectioning possibility introduced by cluster projectile ions, such applications are only possible in combination with freeze−fracture techniques that arbitrarily expose portions of the cells to mass spectral surface analysis. Even in this case, however, surface coverage layers of pure ice may be created during the fracture process that impose large problems to the subsequent static surface analysis. As demonstrated above, these layers can easily be removed using polyatomic ion beams. An important feature of the technique is the finding that the static SIMS or neutral molecule surface analysis following a sputtering cycle can be performed with atomic Ga^+ ions as well as with the eroding C_{60}^+ beam itself. As a consequence, it is possible to utilize the high spatial resolution of the Ga^+ ion beam for molecular three-dimensional imaging applications. This finding is of particular importance since it does not yet seem feasible to increase the focusing properties of the C_{60}^+ ion source to a level routinely achieved by liquid metal ion sources.

(25) Winterbon, K. B.; Sigmund, P.; Sanders, J. B. *K. Dansk. Vid. Selsk.* **1970**, *37*, 5−61.
(26) Stapel, D.; Benninghoven, A. *Appl. Surf. Sci.* **2001**, *174*, 261−270.
(27) Fuoco, E. R.; Gillen, G.; Wijesundara, M. B. J.; Muthu, B. J.; Wallace, W. E.; Hanley, L. *J. Phys. Chem. B* **2001**, *105*, 3950−3956.
(28) Ghalab, S.; Staudt, C.; Maksimov, S. E.; Mazarov, P.; Tugushev, V. I.; Dzhemilev, N. Kh.; Wucher, A. *Nucl. Instrum. Methods B* **2002**, *197*, 43−48.

ACKNOWLEDGMENT

The authors gratefully acknowledge the financial support of the National Science Foundation and the National Institutes of Health.

Received for review March 5, 2004. Accepted September 9, 2004.

AC049641T